In tumors *Salmonella* migrate away from vasculature toward the transition zone and induce apoptosis

Sabha Ganai[1,2], **Richard B. Arenas**[1,2,3], **Jeremy P. Sauer**[4], **Brooke Bentley**[3], and **Neil S. Forbes**[2,3,4,*]

[1] Department of Surgery, Baystate Medical Center / Tufts University School of Medicine, Springfield, Massachusetts

[2] Program in Molecular and Cellular Biology, University of Massachusetts Amherst, Amherst, Massachusetts

[3] Pioneer Valley Life Sciences Institute, Springfield, Massachusetts

[4] Department of Chemical Engineering, University of Massachusetts Amherst, Amherst, Massachusetts

Abstract

Motile bacteria can overcome diffusion resistances that substantially reduce the efficacy of standard cancer therapies. Many reports have also recently described the ability of *Salmonella* to deliver therapeutic molecules to tumors. Despite this potential, little is known about the spatiotemporal dynamics of bacterial accumulation in solid tumors. Ultimately this timing will affect how these microbes are used therapeutically. To determine how bacteria localize, we intravenously injected *Salmonella typhimurium* into BALB/c mice with 4T1 mammary carcinoma and measured the average bacterial content as a function of time. Immunohistochemistry was used to measure the extent of apoptosis; the average distance of bacteria from tumor vasculature; and the location of bacteria in four different regions: the core, transition, body and edge. Bacteria accumulation was also measured in pulmonary and hepatic metastases. The doubling time of bacterial colonies in tumors was measured to be 16.8 hours, and colonization was determined to delay tumor growth by 48 hours. From 12 and 48 hours after injection, the average distance between bacterial colonies and functional vasculature significantly increased from 130 to 310μm. After 48 hours, bacteria migrated away from the tumor edge toward the central core and induced apoptosis. After 96 hours, bacteria began to marginate to the tumor transition zone. All observed metastases contained *Salmonella* and the extent of bacterial co-localization with metastatic tissue was 44% compared to 0.5% with normal liver parenchyma. These results demonstrate that *Salmonella* can penetrate tumor tissue and can selectively target metastases, two critical characteristics of a targeted cancer therapeutic.

*Corresponding Author: Neil S. Forbes, Ph.D., Department of Chemical Engineering, University of Massachusetts Amherst, 101 Goessmann Laboratory, 686 North Pleasant Street, Amherst, MA 01003, 413-577-0132 (office), 413-545-1647 (FAX), forbes@ecs.umass.edu.

Keywords

Bacteriolytic Therapy; Attenuated *Salmonella typhimurium*; Tumor Transition Zone; Apoptosis; Metastases

---

Introduction

Microenvironment heterogeneity is a significant obstacle in the clinical management of advanced tumors[1]. As a consequence of aberrant cellular proliferation and neoangiogenesis, solid tumors exhibit anomalous vascular structures and cellular environments that lead to resistance to standard therapies[2–3]. Disorganized vascular architecture increases the diffusion distance of blood-borne chemotherapeutics, spatially compromising their efficacy[4]. The tumor microenvironment also influences the physiology of cancer cells and their sensitivity to treatment[5–6]. Hypoxia selects for apoptosis-resistant and p53-deficient cell types, which promotes subpopulations of cancer cells that have resilience to cytotoxic agents[7–9]. On the tissue length scale, cells in the tumor transition zone are diffusion-limited, hypoxic and p53-resistant[10], increasing their resistance to therapy. The transition zone is a region of cellular quiescence at the margin of viable and dead tumor cells that histologically has fewer mitotic figures and a different stromal density than viable tumor tissue[10]. In addition, the transition zone is a morphologic finding associated with host cachexia and tumor aggressiveness[10].

Metastatic disease is the leading cause of cancer-related death in breast cancer and other solid tumors[9]. While metastases are typically organ-specific, they are often located in numerous sites secondary to systemic embolization, making specificity in localization and delivery towards metastases an important therapeutic goal. Any modality that can effectively target tumors while avoiding toxicity to normal tissue would be ideal as an anti-metastatic therapy.

Therapeutic bacteria have the potential to overcome transport limitations in tumors and specifically target metastases. Capitalization of the innate motility and genetic machinery of bacteria has broadened their scope as a cancer therapeutic, allowing for their potential use as intrinsically cytotoxic agents, as well as vectors for the programmed delivery of cytotoxic proteins into tumors[11–14]. Attenuated strains of *Salmonella typhimurium*, which are intrinsic motility, have been shown to preferentially accumulate within tumors[15–18] and target specific microenvironments[19]. Following systemic injection, *S. typhimurium* accumulate in the dying tissue of mouse mammary tumors[16]. More specifically, *E. coli* strain Nissle 1917 (a facultative anaerobe similar to *S. typhimurium*) has been shown to accumulate in the region between viable and necrotic tissue[20–21]. Using tumor cylindroids it was shown that *S. typhimurium* accumulation within tumors is dependent the presence of necrotic and quiescent microenvironments[22]. In addition, bacterial accumulation within regions of quiescence has been shown to be dependent on chemotaxis receptors[23]. Once colonized, *S. typhimurium* induce apoptosis[23]. Phase I clinical trials have demonstrated limited accumulation of *S. typhimurium*[24–25], suggesting that improved understanding is necessary to perfect their targeting ability.

To examine the spatiotemporal dynamics of bacterial accumulation within tumors we quantified the localization of non-pathogenic *S. typhimurium* in syngeneic mammary tumors in immunocompetent mice. We hypothesized that, 1) *after intravenous injection*, *S. typhimurium would migrate away from perfused vasculature towards regions of dying cells,* 2) *bacterial accumulation within tumors would be associated with an induction of apoptosis*, and 3) *S. typhimurium would accumulate in both microscopic and macroscopic metastases*. To test these hypotheses the accumulation of bacteria within tumors was compared to accumulation liver over time and tumor volume was measured. Bacterial localization to regions of apoptosis and necrosis was assessed by immunohistochemistry as a function of time. In addition, bacterial patterns of accumulation relative to vasculature were classified and the extent of bacterially induced apoptosis was measured. Finally, *Salmonella* immunohistochemistry was used to identify bacterial accumulation in hepatic and pulmonary metastases.

MATERIALS AND METHODS

Cell Lines and Reagents

4T1 mammary carcinoma cells (American Tissue Type Collection; Manassas, VA) were maintained at 37°C, 5% CO_2 in RPMI-1640 with 10% fetal bovine serum. Trypsinized cells were resuspended in phosphate-buffered saline (PBS) at 5×10^6 cells/ml immediately prior to use. The *msbB⁻ purI⁻ xyl⁻ Salmonella typhimurium*, strain VNP20009 (Vion Pharmaceuticals; New Haven, CT), was grown in Luria-Bertani (LB) media at 37°C until mid-log phase prior to resuspension in PBS at 10^7 cfu/ml. Biotinylated *Lycopersicon esculenatum* (tomato) lectin (Vector Laboratories; Burlingame, CA) was reconstituted in sterile water at 2 mg/ml for use as a perfusion stain. Immunohistochemical reagents were obtained from Dako (Carpinteria, CA), unless otherwise noted.

Syngeneic Murine Tumor Model

Animal care was conducted in accordance with the National Institute of Health guidelines for care and use of laboratory animals. Prior approval from the Baystate Medical Center Institutional Animal Care and Use Committee was obtained. At 8–12 weeks of age, Balb/c mice received a subcutaneous injection of 50,000 4T1 cells using a 10μl Hamilton syringe at the level of the right third mammary fat pad. Tumor volume was estimated with measurements obtained from an electronic vernier caliper using the equation *(length)(width)(height)π/6*. Tumor mass was determined at the time of necropsy. After tumor implantation, 4T1 cells rapidly form liver and lungs metastases, typically within three to four weeks[26].

Experimental Treatments

After 21 days of 4T1 tumor growth, mice received systemic injection via tail vein with 100,000 colony forming units (cfu)/g VNP20009 or PBS (control). At predetermined time points, mice were injected with the 5 mg/kg biotinylated tomato lectin perfusion stain, followed by euthanasia after an interval of five minutes[16]. In mice administered bacteria for six days, necropsies were performed and liver and lung samples were fixed in 10% neutral buffered formalin.

Tissue Bacterial Content

Tumor and liver samples were weighed then minced in a known volume of PBS until homogenous, followed by plating of serial dilutions on LB agar. After 24–48 hours incubation at 37°C, colony forming units were counted to determine bacterial concentration (cfu/g) as described previously[16].

Histology

Tumors were fixed in 10% neutral buffered formalin, then processed and embedded in paraffin. Oriented, sequential, 4μm sections of equatorial tumor regions were obtained for standard and immunohistochemical staining. Hematoxylin and eosin (H&E) stains were performed for identification of tissue morphology and necrosis. Antigen retrieval was performed on rehydrated tissue sections using an EZ Retriever System with CitraPlus Antigen Retrieval Solution (BioGenex; San Ramon, CA) in preparation for immunohistochemical staining for cleaved caspase-3 (apoptosis), Salmonella, and/or biotinylated tomato lectin (perfused vasculature).

Cleaved Caspase-3 Immunohistochemistry

A DakoCytomation autostainer was programmed according to manufacturer's settings using a LSAB2 System with horseradish peroxidase (HRP). After a blocking step, sections were incubated in a 1:100 dilution of cleaved caspase-3 monoclonal rabbit antibody (Cell Signaling, Danvers, MA) in 0.2% bovine serum albumin (BSA) for 60 minutes. Envision+ HRP-conjugated anti-rabbit reagent was applied for 30 minutes, followed by staining with DAB+ Chromagen. Sections were counterstained with hematoxylin. Negative controls were performed with omission of the primary antibody.

Salmonella / Perfused Vasculature Dual-Label Immunohistochemistry

A DakoCytomation autostainer was programmed according to manufacturer's settings using an Envision G/2 AP Doublestain System. Sections were incubated in ChemMate avidin-biotin complex for 30 minutes, followed by staining with DAB+ chromagen. After a blocking step, sections were incubated in a 1:200 dilution of rabbit polyclonal antibody to *Salmonella* (Abcam; Cambridge, MA) in 0.2% BSA for 30 minutes. An alkaline phosphatase polymer was applied for 30 minutes, followed by staining with permanent red. Sections were counterstained with hematoxylin. Negative controls were performed with omission of the primary antibody and on a tumor harvested without the tomato lectin perfusion stain. Positive controls were performed on a tumor with intratumoral injection of *S. typhimurium*.

Image Acquisition

An Olympus IX71 Inverted Epi-fluorescence Microscope equipped with a 10X Plan-APO objective, a Ludl Motorized Z-Stage, a monochromatic Hamamatsu cooled-CCD Digital Camera, and a CRI MicroColor trichromatic filter was used to acquire images from immunohistochemically-labeled slides. A script in IPLab (BD Biosciences, Rockville, MD) was used to automate image acquisition and assemble a tiled montage of individual images

comprising three RGB channels, creating macroscopic composite color images of entire tumor sections.

Classification of tumor regions

A randomizing algorithm was used to select thirty individual images ($833.49 \times 635.04\mu m$) per tumor for analysis. Images comprising tissue folds or >25% blank space were excluded. Images were analyzed from slides prepared for dual-labeled immunohistochemistry of bacteria and vasculature, and compared with sequential sections stained for cleaved caspase-3 and H&E. Based on location within the tumor, images were classified as one of four region types: edge (within 1mm of tumor border), core (necrotic center in H&E section), body (viable tumor tissue), and transition zone (border between body and core). Based on histologic evidence of pyknosis, nuclear condensation, and cleaved caspase-3 positivity, images were scored for the presence or absence of apoptosis. All other regions were classified as necrotic or viable based on H&E staining. Bacterial density was determined by counting the number of stained pixels per immunohistochemical image.

Morphometric Analysis

Quantitative image analysis of bacteria and vasculature was performed using ImageJ software (National Institutes of Health). Identical settings were used for all images analyzed per slide. To create a vascular map, the blue channel was conservatively thresholded according to grayscale intensity using a 2% band-width filter, eroded, then binned 25%, allowing capture of brown-stained (DAB+) perfused vasculature in a binary raster file. The green channel was thresholded using a 25–30% low-pass filter, then binned 25%, allowing capture of red-stained *S. typhimurium* and brown-stained vasculature in a binary raster file. Using Euclidean distance matrix analysis27, a 32-bit distance map of the blue channel raster file was created, assigning each pixel a magnitude in proportion to its distance from perfused vasculature. This matrix was multiplied with the green channel raster file, creating a 32-bit bacterial map (vascular space was eliminated via multiplication with zero distance), with pixels representing bacteria having an attributed magnitude in proportion to their distance from vasculature. Using a histogram function for each image, the mean and maximum distances of bacteria from vasculature were acquired, as well as a pixel count representative of bacterial density. Scale calibration was performed using a 10μm slide micrometer.

In liver and lung sections morphometric image analysis was used to determine cross-sectional area of metastases and relative proportion of pixels stained for bacteria using identical thresholding of blue-channel raster files.

Statistical Analysis

Results of image analysis were stratified by microenvironment and summarized per tumor. Descriptive statistics were performed, analyzing a minimum of three tumors per time point. Data are reported as means with 95% confidence intervals (CI) in parentheses. Hypothesis testing was conducted using Student's t-test with two-tailed analysis, with statistical significance assigned at P<0.05.

RESULTS

S. typhimurium preferentially colonized tumors and delayed tumor growth

Following systemic inoculation, an immediate tropism of *S. typhimurium* was observed towards subcutaneous mammary tumors (Figure 1). Tumor bacterial density at 3 hours after inoculation was significantly greater than zero (P<0.05) and increased significantly until hour 12 (P<0.05; Figure 1A). Bacteria preferentially colonized mammary tumors compared to livers (Figure 1A). Averaging all time points, bacteria concentrations were approximately 5000 times greater in tumor than livers; the average bacterial concentrations were 2.6×10^6 cfu/g (95% CI, $8.7 \times 10^4 - 5.2 \times 10^6$ cfu/g) in tumor compared to 477 cfu/g (95% CI, 0 – 980 cfu/g) in liver (p<0.05). All mice demonstrated colonization of tumors, whereas only 65% of liver samples had detectable bacterial colonies. The extent of bacterial colonization increased exponentially with time (*t*, hours), with doubling times of 16.8h (95% CI, 12.5 – 25.6 h) in tumors and 11.2h (95% CI, 9.8 – 13.3 h) in liver. Treatment with *S. typhimurium* delayed tumor growth by approximately 48 hours (Figure 1B). At the time of treatment (21 days of growth) most tumors were large, vascular, and highly necrotic. The mean tumor volume was 1291.3 mm^3 (95% CI, 1045.9 – 1536.7 mm^3) and the maximal (craniocaudal) dimension was 17.74mm (95% CI, 16.42 – 19.06mm). There was a significant difference in tumor volume between treatment groups at both 48 and 144 hours (P<0.05).

S. typhimurium accumulated in the tumor transition zone

Composite images were generated for all tumors to observer macroscopic bacterial behavior (Figure 2A). Immunohistochemical staining identified regions of *Salmonella* accumulation (red in Figure 2, left), functional vasculature (brown in Figure 2A, left), and apoptosis (brown in Figure 2A, middle). Negative controls without primary antibody and without tomato lectin perfusion confirmed stain specificity for functional vasculature. Positive controls performed on tumors with intratumoral injections of *Salmonella* confirmed the specificity of the antibody stain.

The morphology of all observed tumors was highly similar; all tumors contained central necrosis devoid of vessels and a highly vascularized edge (Figure 2A). Tumors were supplied by a primary vascular pedicle entering the medial/peritoneal aspect and numerous smaller vessels supplied the subcutaneous tissues penetrating the lateral/superficial aspect. Based on these conserved characteristics, we defined four discrete tumor regions: 1) a necrotic core, 2) an edge region, 3) viable tissue in the body of the tumor, and 4) a transition zone between the core and the body (Figure 2A, right).

After administration, bacteria were observed in all tumor regions (Figure 2B). Bacteria accumulated as colonies and dispersed throughout the extracellular space (Figure 2B). Intracellular bacterial accumulation was also observed (Figure 2B, right). The relative accumulation in each region changed with time (Figure 2C). At 12 hours, there was preferential accumulation within the edge of tumors (P<0.05). At 48 hours, there was greater bacterial density in all regions and bacteria remained localized at the edge compared to the tumor body and transition zone (p<0.05). At 96 hours, bacterial density decreased within all microenvironments except the transition zone, which increased significantly (p<0.05). This

preference for the transition zone was seen as bands of bacteria around tumor necrosis (Figure 2D).

S. typhimurium induced apoptosis in tumors

Based on imaging of activated caspase-3, more apoptosis was present in bacterially treated tumors compared to controls (Figure 3). To quantify the change in viability following bacterial injection, individual tiles in composite tumor images (Figure 3A) were scored as either apoptotic, necrotic, or viable (Figure 3B). At 48 hours after injection there was significantly more apoptosis and less viable tissue compared to PBS controls ($p < 0.05$; Figure 3B). The trend towards increased apoptosis at 12 hours and its abrogation by 96 hours suggest that the observed delay in tumor growth within the first 48 hours of infection (Figure 1B) was mediated by an induction of apoptosis. The increase in apoptosis was regionally specific. More apoptosis was present in the transition and cores regions at 48 hours compared to controls ($p < 0.05$; Figure 3C). The induction of apoptosis in the transition zone was correlated with bacterial accumulation; colocalization of bacteria with apoptosis was highest in the tumor transition zone where it was significantly greater than the edge ($p < 0.05$, Figure 3D).

Salmonella accumulation migrated away from vasculature

Dual labeled immunohistochemistry was used to determine bacterial localization relative to tumor vasculature (Figure 4A). In thirty images per tumor, the location of bacterial colonies (stained red, white arrow) and functional vasculature (stained brown, black arrow) were concurrently identified (Figure 4A, upper left) and translated into binary images (Figure 4A, upper right). Euclidean distance maps (Figure 4A, lower left) were combined with bacterial binary images to determine the distance of each bacterial colony to the nearest blood vessel (Figure 4A, lower right). In all treated tumors the mean distance between bacteria and vasculature increased from 128.5μm (95% CI, 92.1 – 164.9μm) to 309.0μm (95% CI, 262.0 – 356.0μm) from 12 to 48 hours ($p < 0.05$), followed by a downward inflection at 96 hours (Figure 4B). From these values, bacterial velocity through tumors for the first 48 hours was 6.1 μm/h (95% CI, 4.8 – 7.4 μm/h), which is considerably slower than the linear velocity of motile bacteria in culture medium (20–50μm/s). The average distance at all three time points was significantly greater than zero ($p < 0.05$), suggesting migration from vessels into tumor tissue.

The maximum distance of bacteria from perfused vasculature was dependent on local microenvironment (Figure 4C). In all regions the maximum distance increased between 0, 12 and 48 hours. At the time of injection (0 hr) all bacteria were in the blood plasma, i.e. 0 μm. Two patterns of bacterial migration were observed (Figure 4C): 1) a high initial maximum distance followed by a minimal increase with time, which was observed in the transition and core regions; and 2) a low initial maximum distance that increased rapidly between 12 and 48 hours, which was observed in the edge and body regions. At 12 hours the maximum distance was greater in the core compared to the edge ($p < 0.05$), suggesting that bacteria were able to move rapidly in the necrotic tissue of the core. In the edge, the maximum distance was greater at 48 hours compared to 12 hours ($p < 0.01$), suggesting migration away from the edge and into the tumor with time.

Salmonella specifically targeted breast cancer metastases following systemic administration

Six days after inoculation, gross metastases were observed in all livers, and microscopic metastases were observed in all lungs. On examination with Salmonella immunohistochemistry, colonization was noted within every macroscopic hepatic metastasis and numerous microscopic pulmonary metastases (Figure 5). Hepatic metastases had a mean diameter of 2.6mm (95% CI, 2.1 – 3.1mm) and cross-sectional area of 5.3mm^2 (95% CI, 3.9 – 6.7 mm^2; Figure 5A). Liver metastases had bacterial colonization in 44% (95% CI, 24 – 64%) of their cross-sectional area, compared to 0.5% (95% CI, 0 – 1.2%; P<0.05) within normal hepatic parenchyma, demonstrating tissue specificity towards metastatic cancer tissue (Figure 5B).

Based on immunohistochemical staining, *Salmonella* were present within perivascular pulmonary metastases less than five cells in thickness (Figure 5D), but could not be identified within normal pulmonary tissue. Most observed pulmonary micro-metastases encased vascular channels (Figure 5C), a phenomenon which has been suggested to precede extravasation [28]. Several of these lesions were surrounded by a neutrophilic infiltrate, suggesting initiation of an inflammatory response against tumor and/or bacteria.

DISCUSSION

Bacterial growth and tumor delay

The observed patterns of bacterial accumulation in tumors indicate how bacteria could be used therapeutically. The exponentially growth of *S. typhimurium* in tumors (Figure 1) shows that preferential growth is a key mechanism of bacterial accumulation in tumors and suggests a time schedule for how therapeutic bacteria could be used. We have recently shown that *S. typhimurium* can be engineered to produce cytotoxic agents with externally controlled timing of expression[11]. To achieve maximum efficiency, drug release should be triggered when the density difference between tumor and liver is greatest or at least 3 days (Figure 1A).

The timing of bacterial accumulation (Figure 1A) and tumor growth (Figure 1B) suggests that arming bacteria to produce cytotoxic agents[11–14] will greatly increase their efficacy. After the delay during the initial 48 hours (Figure 1B), tumors resume exponential growth despite continued increase in bacterial density (Figure 1A). A similar delay has been reported previously[29–30]. This delay and the concurrent induction of apoptosis (Figure 3) suggest that bacteria slow tumor growth by inducing apoptosis, but tumors eventually escape and apoptosis abates by 96 hours (Figures 1B and 3B). Bacteria could have induced apoptosis by multiple mechanisms including competition for extracellular nutrients[31], stimulation of immune cells[32–33], or induction of apoptotic signal transduction pathways following intracellular accumulation (Figure 2B, right). The limited time scale of apoptosis induction suggests that a controllably cytotoxic *S. typhimurium*[11] would reduce tumor volume beyond 48 hours.

Over the timescale of these observations (6 days), Salmonella grew exponentially. If this pattern continued, uncontrolled growth could present a risk for sepsis in the clinical setting.

Previous studies in cynomolgus monkeys have shown that systemically injected *Salmonella* are cleared from most organs by 30 days15. It has also been shown in mice that by 14 days following administration *Salmonella* have completely cleared from the liver and tumors densities have stabilized34, suggesting that exponential growth does not persist indefinitely. In addition, the use of an attenuated strain would reduce the risk of sepsis. For example, the *msbB*⁻ mutant investigated here (VNP20009), has been shown to induce considerably less TNF, the primary sepsis stimulating cytokine, than wild type *Salmonella*30."

Spatiotemporal dynamics of bacterial accumulation in tumor microenvironments

The observed accumulation patterns (Figure 2) suggest how *S. typhimurium* localize within tumor microenvironments (Figure 6). Initial localization to the tumor edge (Figure 2C) suggests that systemically injected *S. typhimurium* enter via perfused vasculature at the periphery (Figure 6A) and disseminate during the first 12 hours (Figure 6B). This leads to migration throughout the tumor, with increased accumulation within all microenvironments during the first 48 hours (Figure 6C). Subsequently, the bacteria marginate, leading to preferential accumulation within the tumor transition zone at 96 hours (Figure 6D).

The preferential migration of *S. typhimurium* to the tumor transition zone (Figures 2&6) is important because this region is resistant to therapy10. Preferential trafficking to the transition zone is controlled by chemotaxis to small molecules produced by dying cells at the border of necrosis22. We have previously shown that *S. typhimurium* migration is dependent on aspartate, serine and ribose gradients produced by tumors23. Competition for nutrients in this region may also increase the rate of necrosis formation. The rapid increase in partitioning to the transition zone at 96 hours (Figure 2C) suggests this may be the optimal time to induce cytotoxic protein expression. In all tumors the mean distance between bacteria and perfused vasculature exceeds 100μm (Figure 4) enabling specific targeting to diffusion-limited cancer cells4.

Bacterial migration from tumor vasculature

The rapid migration of *S. typhimurium* away from tumor vasculature addresses previously unanswered questions about the mechanisms of bacterial accumulation in tumors. We previously observed that *S. typhimurium* accumulated in tumor necrosis following systemic injection and speculated that *S. typhimurium* either 1) actively penetrated tumor tissue or 2) induced cell death16. Induction of endothelial cell apoptosis would prune active blood vessels and increase the observed distance between bacteria and vessels. The spatiotemporal results reported here suggest that both of these mechanisms are active: in 4T1 tumors *S. typhimurium* migrated away from vasculature with time (Figure 4B) and induced apoptosis (Figure 3B). However, the timing of these results suggests that the mechanisms are independent. The average distance from vasculature was significantly greater than zero at 12 hours (p<0.05) and the extent of bacterial induced apoptosis was not significant until 48 hours (Figure 3B). This delay suggests that *S. typhimurium* actively extravasated into the tumor interstitium shortly after injection and only induced cell death once colonized. These characteristics are therapeutically relevant because they imply that *S. typhimurium* can be utilized both as a delivery vehicle and as an instrument to induce cancer cell death.

Salmonella targeting of metastases

The presence of *S. typhimurium* in both macroscopic and microscopic metastases (Figure 5) provides additional evidence that accumulation is controlled by gradients of small biological molecules. *In vitro*, we have shown that molecular gradients attract *S. typhimurium* to small tumor masses less than 300μm in diameter22 The ability of *S. typhimurium* to accumulate in small, viable metastases is therapeutically important because it enables targeting of dispersed cancer cells that are typically difficult to treat. Targeting by mechanisms independent of hypoxia gives *S. typhimurium* a significant advantage over obligate anaerobes for targeting metastases1, 35.

These results demonstrate three characteristics of *S. typhimurium* that could be exploited to generate effective anti-cancer therapies: 1) preferential accumulation in the tumor transition zone, 2) ability to rapidly extravasate from tumor vasculature, and 3) preferential accumulation in metastatic lesions. With careful engineering, *S. typhimurium* could be modified to control tumor growth, image cancer throughout the body and eliminate metastases.

Acknowledgments

References

1. Sporn MB. The war on cancer. Lancet. 1996; 347(9012):1377–81. [PubMed: 8637346]

2. Cairns R, Papandreou I, Denko N. Overcoming physiologic barriers to cancer treatment by molecularly targeting the tumor microenvironment. Mol Cancer Res. 2006; 4(2):61–70. [PubMed: 16513837]

3. Jain RK, Forbes NS. Can engineered bacteria help control cancer? Proc Natl Acad Sci U S A. 2001; 98(26):14748–50. [PubMed: 11752416]

4. Minchinton AI, Tannock IF. Drug penetration in solid tumours. Nat Rev Cancer. 2006; 6(8):583–92. [PubMed: 16862189]

5. Albini A, Sporn MB. The tumour microenvironment as a target for chemoprevention. Nat Rev Cancer. 2007; 7(2):139–47. [PubMed: 17218951]

6. Sung SY, Hsieh CL, Wu D, Chung LW, Johnstone PA. Tumor microenvironment promotes cancer progression, metastasis, and therapeutic resistance. Curr Probl Cancer. 2007; 31(2):36–100. [PubMed: 17362788]

7. Graeber TG, Osmanian C, Jacks T, Housman DE, Koch CJ, Lowe SW, et al. Hypoxia-mediated selection of cells with diminished apoptotic potential in solid tumours. Nature. 1996; 379(6560):88–91. [PubMed: 8538748]

8. Vaupel P, Harrison L. Tumor hypoxia: causative factors, compensatory mechanisms, and cellular response. Oncologist. 2004; 9 (Suppl 5):4–9. [PubMed: 15591417]

9. Yu JL, Rak JW, Coomber BL, Hicklin DJ, Kerbel RS. Effect of p53 status on tumor response to antiangiogenic therapy. Science. 2002; 295(5559):1526–8. [PubMed: 11859195]

10. Bustuoabad OD, Ruggiero RA, di Gianni P, Lombardi MG, Belli C, Camerano GV, et al. Tumor transition zone: a putative new morphological and functional hallmark of tumor aggressiveness. Oncol Res. 2005; 15(3):169–82. [PubMed: 16050138]

11. Ganai S, Arenas RB, Forbes NS. Tumour-targeted delivery of TRAIL using Salmonella typhimurium enhances breast cancer survival in mice. Br J Cancer. 2009; 101(10):1683–91. [PubMed: 19861961]

12. Jiang SN, Phan TX, Nam TK, Nguyen VH, Kim HS, Bom HS, et al. Inhibition of Tumor Growth and Metastasis by a Combination of Escherichia coli-mediated Cytolytic Therapy and Radiotherapy. Mol Ther. 2010

13. Loeffler M, Le'Negrate G, Krajewska M, Reed JC. Inhibition of tumor growth using salmonella expressing Fas ligand. J Natl Cancer Inst. 2008; 100(15):1113–6. [PubMed: 18664657]

14. Ryan RM, Green J, Williams PJ, Tazzyman S, Hunt S, Harmey JH, et al. Bacterial delivery of a novel cytolysin to hypoxic areas of solid tumors. Gene Ther. 2009; 16 (3):329–39. [PubMed: 19177133]

15. Clairmont C, Lee KC, Pike J, Ittensohn M, Low KB, Pawelek J, et al. Biodistribution and genetic stability of the novel antitumor agent VNP20009, a genetically modified strain of Salmonella typhimurium. J Infect Dis. 2000; 181(6):1996–2002. [PubMed: 10837181]

16. Forbes NS, Munn LL, Fukumura D, Jain RK. Sparse initial entrapment of systemically injected Salmonella typhimurium leads to heterogeneous accumulation within tumors. Cancer Res. 2003; 63(17):5188–93. [PubMed: 14500342]

17. Zhao M, Yang M, Li XM, Jiang P, Baranov E, Li S, et al. Tumor-targeting bacterial therapy with amino acid auxotrophs of GFP-expressing Salmonella typhimurium. Proc Natl Acad Sci U S A. 2005; 102(3):755–60. [PubMed: 15644448]

18. Zhao M, Yang M, Ma H, Li X, Tan X, Li S, et al. Targeted therapy with a Salmonella typhimurium leucine-arginine auxotroph cures orthotopic human breast tumors in nude mice. Cancer Res. 2006; 66(15):7647–52. [PubMed: 16885365]

19. Sznol M, Lin SL, Bermudes D, Zheng LM, King I. Use of preferentially replicating bacteria for the treatment of cancer. J Clin Invest. 2000; 105(8):1027–30. [PubMed: 10772643]

20. Yu YA, Shabahang S, Timiryasova TM, Zhang Q, Beltz R, Gentschev I, et al. Visualization of tumors and metastases in live animals with bacteria and vaccinia virus encoding light-emitting proteins. Nat Biotechnol. 2004; 22(3):313–20. [PubMed: 14990953]

21. Stritzker J, Weibel S, Hill PJ, Oelschlaeger TA, Goebel W, Szalay AA. Tumor-specific colonization, tissue distribution, and gene induction by probiotic Escherichia coli Nissle 1917 in live mice. Int J Med Microbiol. 2007; 297(3):151–62. [PubMed: 17448724]

22. Kasinskas RW, Forbes NS. Salmonella typhimurium specifically chemotax and proliferate in heterogeneous tumor tissue in vitro. Biotechnol Bioeng. 2006; 94(4):710–21. [PubMed: 16470601]

23. Kasinskas RW, Forbes NS. Salmonella typhimurium lacking ribose chemoreceptors localize in tumor quiescence and induce apoptosis. Cancer Res. 2007; 67(7):3201–9. [PubMed: 17409428]

24. Heimann DM, Rosenberg SA. Continuous intravenous administration of live genetically modified salmonella typhimurium in patients with metastatic melanoma. J Immunother. 2003; 26(2):179–80. [PubMed: 12616110]

25. Toso JF, Gill VJ, Hwu P, Marincola FM, Restifo NP, Schwartzentruber DJ, et al. Phase I study of the intravenous administration of attenuated Salmonella typhimurium to patients with metastatic melanoma. J Clin Oncol. 2002; 20(1):142–52. [PubMed: 11773163]

26. Yoneda T, Michigami T, Yi B, Williams PJ, Niewolna M, Hiraga T. Actions of bisphosphonate on bone metastasis in animal models of breast carcinoma. Cancer. 2000; 88(12 Suppl):2979–88. [PubMed: 10898341]

27. Cole TM 3rd, Richtsmeier JT. A simple method for visualization of influential landmarks when using euclidean distance matrix analysis. Am J Phys Anthropol. 1998; 107(3):273–83. [PubMed: 9821492]

28. Wong CW, Song C, Grimes MM, Fu W, Dewhirst MW, Muschel RJ, et al. Intravascular location of breast cancer cells after spontaneous metastasis to the lung. Am J Pathol. 2002; 161(3):749–53. [PubMed: 12213701]

29. Pawelek JM, Low KB, Bermudes D. Tumor-targeted Salmonella as a novel anticancer vector. Cancer Res. 1997; 57(20):4537–44. [PubMed: 9377566]

30. Low KB, Ittensohn M, Le T, Platt J, Sodi S, Amoss M, et al. Lipid A mutant Salmonella with suppressed virulence and TNFalpha induction retain tumor-targeting in vivo. Nat Biotechnol. 1999; 17(1):37–41. [PubMed: 9920266]

31. Kim BJ, Forbes NS. Single-cell analysis demonstrates how nutrient deprivation creates apoptotic and quiescent cell populations in tumor cylindroids. Biotechnol Bioeng. 2008; 101(4):797–810. [PubMed: 18814293]

32. Rosenberg SA, Spiess PJ, Kleiner DE. Antitumor effects in mice of the intravenous injection of attenuated Salmonella typhimurium. Journal of Immunotherapy. 2002; 25(3):218–225. [PubMed: 12000863]

33. Lee CH, Wu CL, Shiau AL. Salmonella choleraesuis as an anticancer agent in a syngeneic model of orthotopic hepatocellular carcinoma. International Journal of Cancer. 2008; 122(4):930–935.

34. Zheng LM, Luo X, Feng M, Li ZJ, Le T, Ittensohn M, et al. Tumor amplified protein expression therapy: Salmonella as a tumor-selective protein delivery vector. Oncology Research. 2000; 12(3): 127–135. [PubMed: 11216671]

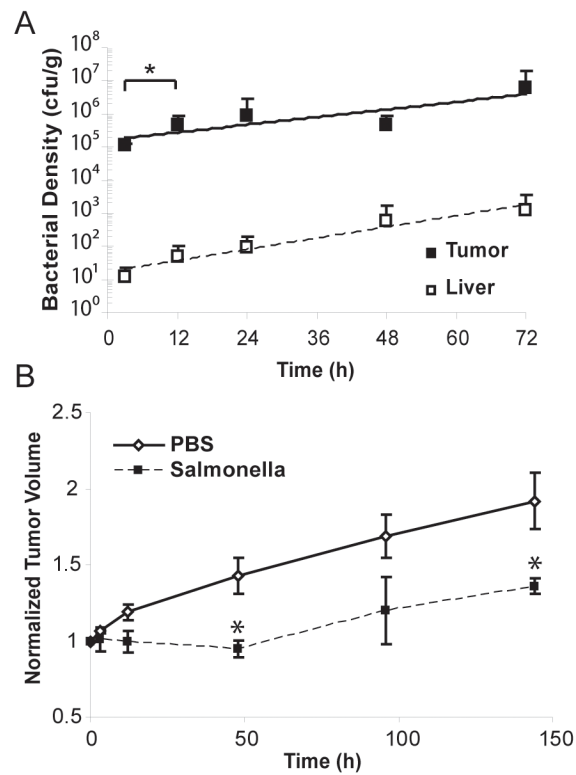35. Forbes NS. Profile of a bacterial tumor killer. Nat Biotechnol. 2006; 24(12):1484–5. [PubMed: 17160044]

Figure 1. *Salmonella* **proliferated exponentially in 4T1 mammary tumors**
A, bacterial density(cfu/g) in tumors and liver samples harvested after systemic injection of
S. typhimurium. Density was greater at 12 hours compared to 3 hours (*, p<0.05).
Exponential growth was observed in both tissues. *B*, Tumor volume was significantly less in
tumors treated with *S. typhimurium* at 48 and 144 hours compared to saline controls (*,
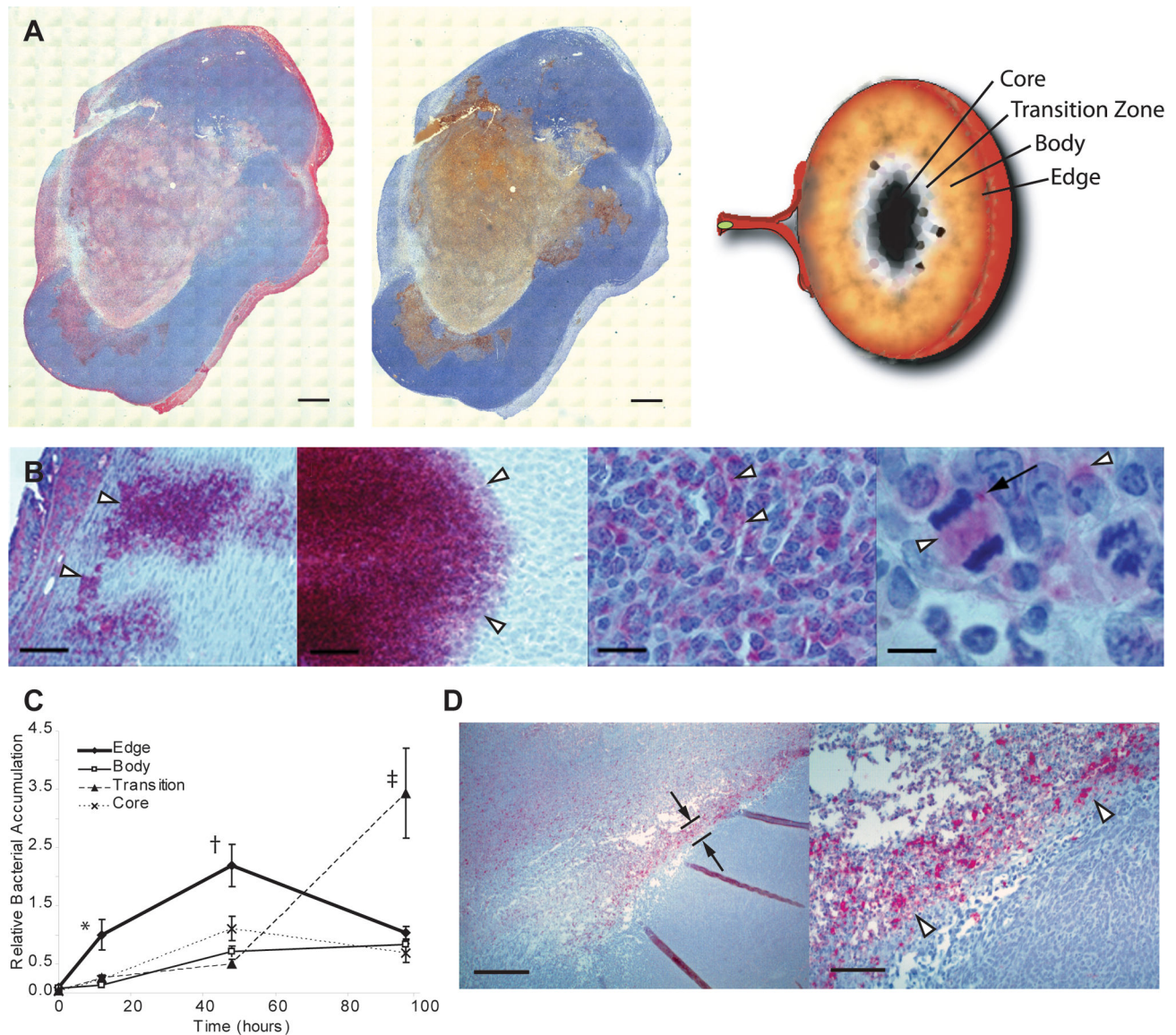p<0.05). Tumor volumes were normalized to initial volume.

Figure 2. *Salmonella* accumulated in distinct tumor regions over time

A, Composite images of 4T1 Tumors, 12 hours after systemic bacterial injection. Serial 4μm sections were dual label stained using a combination of Salmonella immunohistochemistry and biotinylated tomato lectin (left) to visualize bacteria (red) and perfused vasculature (brown) or stained using cleaved caspase-3 immunohistochemistry (middle) to visualize regions of apoptosis (brown). Scale bars are 1mm. Based on histological staining, four regions with distinct microenvironments were observed in each tumor: edge (within 1mm of tumor periphery), body, transition, or core. *B*, *Salmonella* accumulated as colonies in the edge (left) and body (middle left) tumor regions. Bacteria were seen dispersed throughout the extracellular space, shown here in the body region (middle right). Arrows indicate colony edges (left, middle left) and individual bacteria in the extracellular space (middle right). Salmonella were observed both extracellularly and intracellularly (white arrows, right). The black arrow highlights a single extracellular bacterium (right). Scale bars are

50μm (left, middle left), 25μm (middle right), and 10μm (right). *C*, Dynamics of bacterial accumulation were determined by measuring pixel density per image and normalized to the edge microenvironment at 12 hours. At 12 and 48 hours, there was significantly greater accumulation within the edge than all other regions (*, $p < 0.05$; †, $p < 0.01$; except the core at 48 hrs). At 96 hours, there was greater accumulation within the tumor transition zone compared to all other regions (‡, $p < 0.01$). *D,* At late time points *Salmonella* accumulated as stratified bands in the tumor transition zone (between arrows, left and highlighted, right). Arrows indicate boundary of the transition zone. Sparse accumulation in the necrotic core is present in *D*-left. Scale bars are 1mm (left) and 100μm (right).
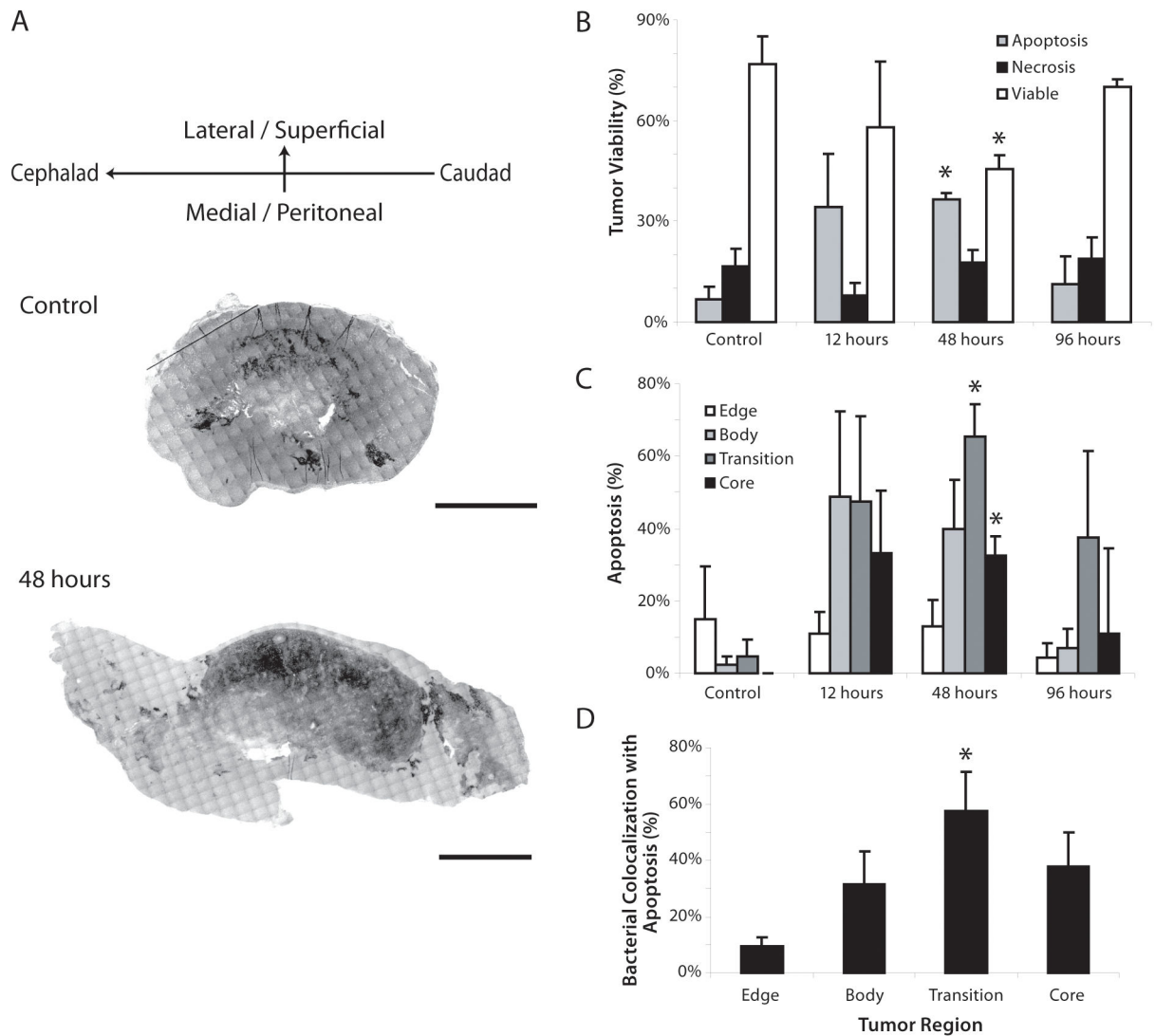
Figure 3. Systemic bacterial injection induced apoptosis in 4T1 tumors
A, Composite images of equatorial tumor sections stained for cleaved caspase-3. Sections were oriented in a coronal plane along craniocaudal and medial/lateral axes, and imaged using the blue channel filter. *B*, Individual images in each tumor composite (as in *A*) were scored as apoptotic, necrotic or viable based on identification of pyknosis, nuclear condensation or cleaved caspase-3. At 48 hours, the extent of apoptosis significantly increased and the extent of viable tissue decreased compared to PBS controls (*, $p<0.05$). No differences were seen in the relative proportion of tumor necrosis. *C,* Significantly more apoptotic tissue was observed 48 hours after injection in the transition and core regions compared to PBS controls (*, $p<0.05$). *D,* For all tumors, greater colocalization of bacteria with apoptosis was seen in the transition zone compared to the edge (*, $p<0.05$).

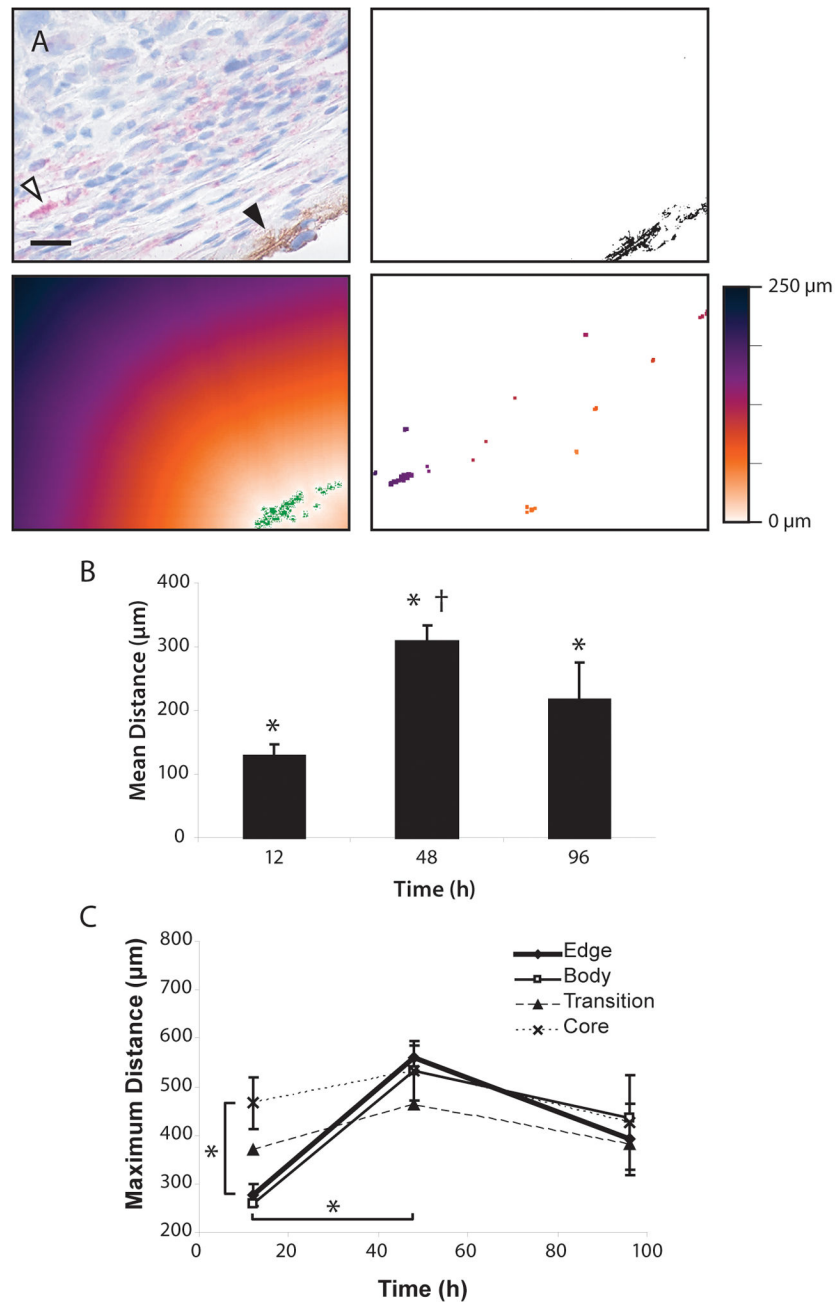**Figure 4. Bacterial accumulation migrated away from vessels with time**

A, The location of *Salmonella* colonies (white arrow, red stain) and perfused blood vessels (black arrow, brown stain) were identified using dual label immunohistochemistry *(upper left)*. The location of vessels was captured from the blue component of the image (*upper right*) and used to generate a Euclidian distance map (*lower left*). Merged distance maps identified the location of bacterial colonies relative to the nearest functional vessel (*lower right*). The mean distance between the colonies and perfused vasculature in this example image is 185.9 ± 67.6 (SD) μm. The scale bar is 25μm. *B*, The mean distance between bacteria and vasculature increased for 48hrs after injection. The distances at 12 and 48 hrs

were greater than zero (*, p<0.05) and increased between 12 and 48hrs (†, p<0.0001). Thirty images were examined per tumor. *C,* Maximum distance of bacteria from vasculature as a function of time, grouped by region. At 12 hours, the maximum distance was greater in the core compared to the edge (*, p<0.05). The maximum distance in the edge increased from 12 to 48 hours (*, p<0.01). For clarity, error bars are only displayed for the edge and core regions.
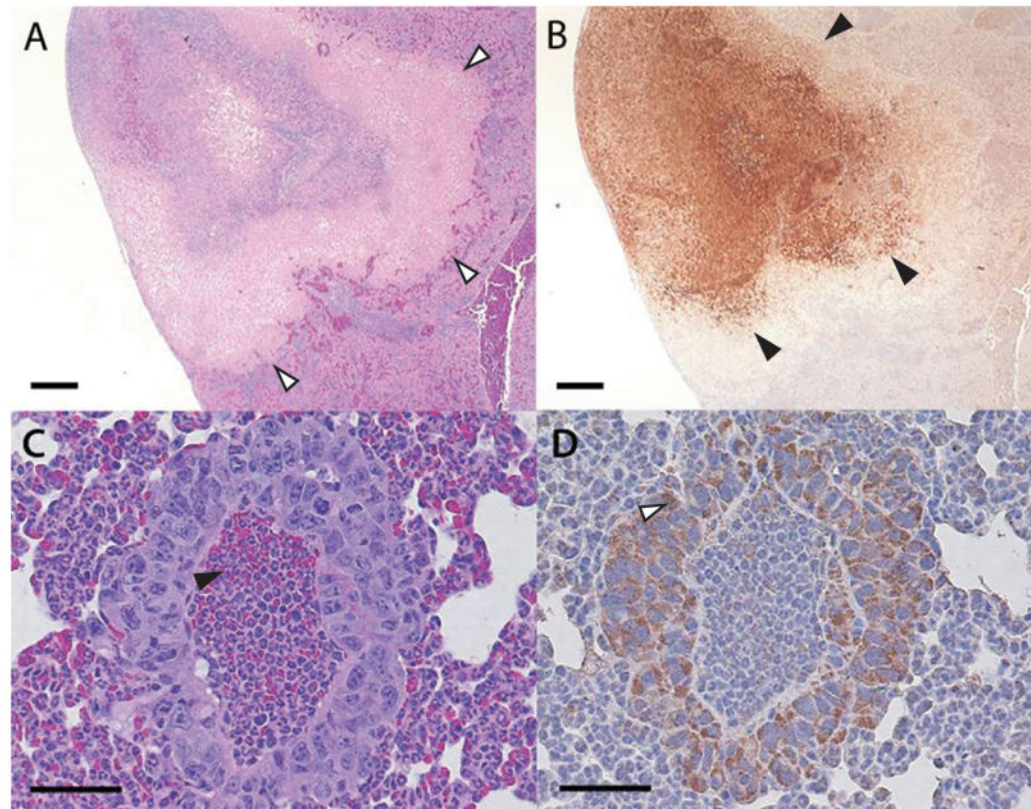
Figure 5. *Salmonella* targets breast cancer metastases
Contiguous hepatic (*A, B*) and pulmonary (*C, D*) sections were stained with hematoxylin and eosin (*A, C*) and Salmonella immunohistochemistry (brown in *B, D*). *A–B*, *Salmonella* accumulated in hepatic metastases with greater specificity than normal liver parenchyma. Bacterial colonies (boundary indicated with dark arrows in *B*) colocalized with metastatic tissue (boundary indicated with white arrows in *A*). Scale bars are 250μm. *C–D*, *Salmonella* (e.g. white arrow) accumulated in small pulmonary micro-metastases. The micro-metastasis encased a vascular channel containing an inflammatory infiltrate (black arrow). Scale bars are 50μm.
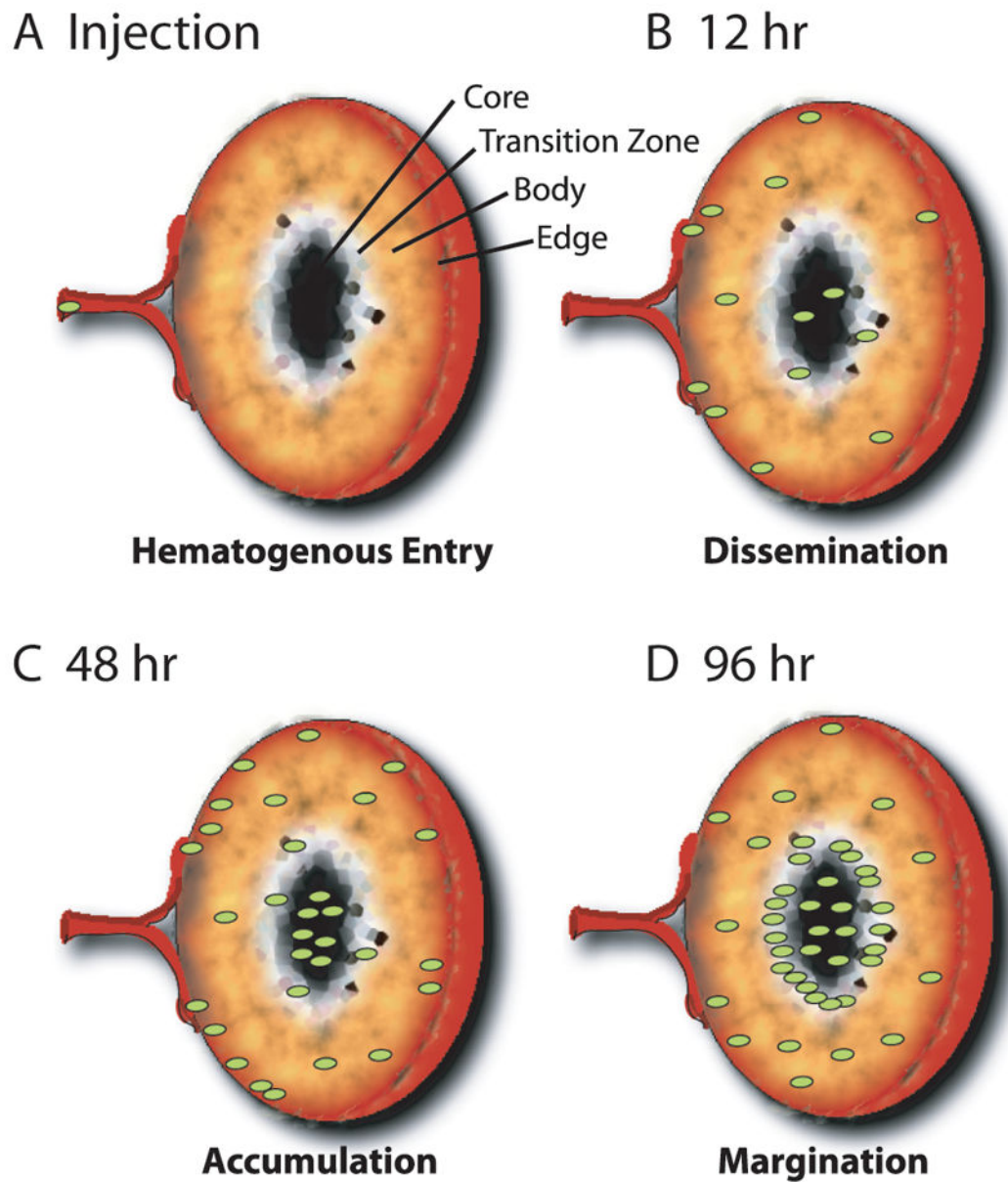
Figure 6. Model of *Salmonella* accumulation within tumor microenvironments
A) Bacteria first access the tumor via hematogenous entry. *B*) During the first 12 hours bacteria disseminate throughout all microenvironment regions. *C*) For first 48 hours bacteria migrate and proliferate, resulting to accumulation within all regions. *D*) By 96 hours, bacteria marginate to the tumor transition zone and density decreases in other regions.